JOURNAL OF APPLIED ELECTROCHEMISTRY 19 (1989) 69–75

Length distribution of aluminum etch tunnels

THEODORE R. BECK
Electrochemical Technology Corp., 1601 Dexter Ave. N., Seattle, WA 98109, USA

HIDENORI UCHI
KDK Corporation, 363, Arakawa, Takahati-Shi, Ibaraki-Ken 318, Japan

KURT R. HEBERT
Department of Chemical Engineering, Iowa State University, Ames, IA 50011-2230, USA

Received 10 December 1987; revised 18 May 1988

A model was derived for the length distribution of aluminum etch tunnels, based on an assumed constant death rate per unit length. Both active and dead tunnels were accounted. The model gives reasonable fits to measured tunnel length distribution data with two adjustable parameters, the death rate per unit length and the number of active tunnels. The death rate parameter has a value of about 2% of tunnels dying per μm of growth length for the set of experimental data. The numbers of active and dead tunnels appear to be consistent with other tunnel measurements.

Nomenclature

- d depth of field in SEM photograph
- F fraction of tunnels
- i current density ($A\,cm^{-2}$)
- K_D fraction of tunnels dying per unit length (μm^{-1})
- l length of tunnel under consideration (μm)
- Δl length increment (μm)
- L maximum tunnel length from time zero (μm)
- n number of Δl increments
- N number of tunnels per cm^2
- N' number of tunnels per arbitrary area
- t time (s)
- u tunnel velocity ($\mu m\,s^{-1}$)
- w tunnel width (μm or cm)
- ϕ ratio of depth of field to length scanned in SEM

Subscripts

- A active tunnels
- D dead or dying tunnels
- e end of tunnel
- E ends of all active tunnels
- F foil surface
- o initial generation of tunnels
- T total tunnels
- w tunnel wall
- W walls of total number of tunnels

1. Introduction

Tunnel etching of aluminum foil is a commercial process used to increase area and capacitance of electrolytic capacitors. Alwitt *et al.* [1] have recently reviewed the process and presented effects of several parameters on velocity and width.

Tunnel length distribution is an important aspect of the tunnel etch phenomenon that has not previously been treated. Hebert [2] and Alwitt *et al.* [3] have shown that tunnels die when the value of a geometry parameter related to the tunnel length and the taper ratio reaches a critical value. This geometry parameter is linearly related to the steady-state diffusion resistance within tunnels. He gives evidence that the critical transport resistance is that required to give saturation of $AlCl_3$ at the end. On the other hand, examination of scanning electron microscope (SEM) photographs of tunnels shows that they are not of uniform length. Only a small fraction grow to the maximum length corresponding to their constant [2] velocity and the duration of the experiment. Another death mechanism is indicated for the shorter tunnels.

A model is derived here, based on a continuous death mechanism, relating tunnel length distribution to duration of an experiment, or maximum tunnel length. The model is fitted to experimental SEM data, and death rate parameters are evaluated.

2. Model

The total number of tunnels observed on an SEM photograph is the sum of the number of active tunnels at the time the current was turned off, and the number of tunnels that died from time zero to time of current off.

$$N_T = N_A + N_D \quad (1)$$

Assuming all the current goes to active tunnels, the number of active tunnels can be described by

$$N_A = \frac{i_F}{i_e w^2} \quad (2)$$

Average current density to the foil surface, i_F, is a constant during a galvanostatic experiment and the average current density at the tunnel ends, i_e, is constant for constant tunnel velocity [2]. Tunnel width is reasonably constant with length at temperatures of 60–70° C but at 90° C tunnels taper considerably. For simplicity in the derivation, it is assumed that w is constant in the range 60–80° C for all the longest tunnels. For these conditions, N_A is a constant.

The derivation of the tunnel length distribution function in this paper is based on the assumption that the fraction of tunnels dying per unit time is constant. This fraction is denoted $K_D u$, where u is the constant tunnel growth velocity. Further, if tunnels are selected randomly for death, without preference for certain lengths, the probability of an individual tunnel dying per unit time is also $K_D u$. Thus, K_D, which is the probability of death of an individual tunnel per unit length of its growth, is assumed constant in this work. A constant value for K_D would follow from the concept of a competition between continuing the propagation of a given tunnel or initiating an adjacent new tunnel on the surface of the foil. If propagation is by repeated nucleation of corrosion steps [3] and the ohmic potential drop in a tunnel is small [2], the assumption of a constant K_D is reasonable. Another possible reason for a constant death probability would follow from the mechanism for tunnel growth given by Hebert [2]. According to this mechanism, the ends of all tunnels are poised at a critical potential for passivation, so that tunnels would be chosen randomly for death at a rate which balanced the formation rate of new tunnels. The derivation proceeds on the basis of constant K_D and the final equation is compared to experimental data for evaluation of its validity.

The number of dead tunnels is related to K_D by

$$N_D = N_A + N_A K_D u t \tag{3}$$

in which

$$ut = L \tag{4}$$

the maximum tunnel length. The total number of tunnels is then

$$N_T = N_A + N_A K_D u t \tag{5}$$

In non-dimensional form

$$\frac{N_T}{N_A} = 1 + K_D u t \tag{6}$$

The length distribution function of active tunnels is denoted $F(l, t)$; the fraction of active tunnels at length l, and within a small interval in length Δl, is $F(l, t)\Delta l$. The differential equation for the tunnel length distribution function is derived by consideration of changes, resulting from tunnel growth and death, in the number of active tunnels in a small interval in tunnel length Δl, during a small time interval Δt. In Δt, the fraction of tunnels entering Δl by growth is $uF(l, t)\Delta t$, and the fraction of tunnels leaving by growth is $uF(l + \Delta l, t)\Delta t$. Since K_D is the fraction of tunnels dying per unit length as tunnels grow, the fraction of tunnels which die in Δt is $K_D u \Delta t$. Also, since tunnels are selected randomly for death, the number of tunnels within length interval Δl which die in Δt is proportional to the number of tunnels in that length interval. Thus, the fraction of tunnels dying in Δt in Δl is $K_D u \Delta t F(l, t)\Delta l$. Finally, the accumulation of tunnels within Δl in Δt is $F(l, T + \Delta t)\Delta l - F(l, t)\Delta l$.

The expressions for changes in the distribution function by growth, death and accumulation are formed into a continuity equation for the distribution function.

$$\Delta l[F(l, t + \Delta t) - F(l, t)] = u\Delta t[F(l, t) - F(l + \Delta l, t)] - K_D u F(l, t)\Delta l \Delta t \tag{7}$$

If Δl and Δt are both allowed to approach zero, a differential equation for $F(l, t)$ is formed.

$$\partial F/\partial t + u\partial F/\partial l = -K_D u F \tag{8}$$

This continuity equation is mathematically equivalent to the equation for reactant concentration in a plug-flow chemical reactor with a first-order chemical reaction and no diffusion.

The initial condition for the distribution is

$$F(l, 0) = \delta(l) \tag{9}$$

in which $\delta(l)$ is the Dirac delta function. $\delta(l)$ has a value of ∞ at $l = 0$, and zero elsewhere. Equation 9 represents the tunnels which are assumed to form immediately when the current is first applied in the experiment. By definition of the Dirac delta function, the integral of $\delta(l)$ from $-\infty$ to ∞, which represents all the tunnels in the distribution, is unity, as required. The boundary condition at $l = 0$ is based on continuity of the distribution at $l = 0$. The flux of tunnels in l space at $l = 0$ must be equal to the nucleation rate of new tunnels. The flux at $l = 0$ is $F(0, t)u$. The nucleation rate, which, in order to preserve the current balance, must equal the total rate of tunnel death at all lengths, is $K_D u$. Thus the boundary condition at $l = 0$ is

$$F(0, t) = K_D \tag{10}$$

Equations 8–10 were solved through separate consideration of first, the initial generation of tunnels formed at $t = 0$, and then, all tunnels formed after $t = 0$. The distribution function for the initial generation is determined by the continuity equation, Equation 8, which may be rewritten as

$$DF_0/Dt = -K_D u F_0 \tag{11}$$

in which DF_0/Dt is the substantial derivative of F_0, and is equal to the left side of Equation 8. The substantial derivative refers to changes in number of a particular group of tunnels within a small increment of length, as the tunnels in the group grow and some of them die. Since all the tunnels in F_0 are always at some particular length, it is useful to write Equation 11 in terms of the substantial derivative. In the case under consideration, Equation 11 is integrated with the initial condition, Equation 9, and the boundary condition

$$F_0(0, t) = 0 \tag{12}$$

The solution for F_0 is

$$F_0 = \delta(l - ut) \exp(-K_D ut)$$
$$= \delta(l - ut) \exp(-K_D l) \quad (13)$$

Thus, the tunnels in the initial generation may always be found at $l = ut$, but their number diminishes exponentially with time. The continuity equation for tunnels formed after $t = 0$ is Equation 8, with the boundary condition Equation 10 and the initial condition

$$F_1(l, 0) = 0 \quad (14)$$

The solution, obtained with Laplace transforms, is

$$F_1(l, t) = K_D \exp(-K_D l);\ l < ut$$
$$F_1(l, t) = 0;\ l > ut \quad (15)$$

The total distribution function for active tunnels is $F(l, t) = F_0(l, t) + F_1(l, t)$:

$$F(l, t) = \delta(l - ut) \exp(-K_D l) + K_D \exp(-K_D l);\ l < ut \quad (16)$$
$$F(l, t) = 0;\ l > ut$$

Integrating $F(l, t)$ from $l = 0$ to $l = ut$ gives a result of unity, as expected from the definition of the length distribution function.

The distribution of dead tunnels can be calculated with the active tunnel distribution given above. The rate of production of dead tunnels at length l is

$$\partial F_D/\partial t = K_D u F(l, t) \quad (17)$$

where $F_D(l, t)$ is the distribution function of dead tunnels on a total active tunnel basis. Thus, if $F_D(l, t)$ is integrated from $l = 0$ to $l = \infty$ and then multiplied by the total number of active tunnels, the result would be the total number of dead tunnels. To obtain $F_D(l, t)$, Equation 16 is inserted for $F(l, t)$ in Equation 17, and Equation 17 is integrated with respect to time, with the initial condition at each length l that $F_D(l, l/u) = 0$. This condition arises because the distribution function Equation 16 reaches length l at time l/u. The result for the distribution of dead tunnels is

$$F_D(l, t) = K_D^2 u \exp(-K_D l)(t - l/u) + K_D \exp(-K_D l);\ l \leqslant ut \quad (18)$$
$$F_D(l, t) = 0;\ l > ut$$

The distribution function for comparison with experimental distributions is the combined distribution of both active and dead tunnels, $F_T(l, t) = F(l, t) + F_D(l, t)$:

$$F_T(l, t) = \delta(l - ut) \exp(-K_D l) + K_D \exp(-K_D l)[2 + K_D u(t - l/u)];$$
$$l \leqslant ut \quad (19)$$
$$F_T(l, t) = 0;\ l > ut$$

When $F_T(l, t)$ is integrated from $l = 0$ to $l = ut$, the result is $1 + K_D ut$, which is in agreement with Equation 6.

An example distribution of active and dead tunnels is calculated from Equations 16 and 19 and plotted in Fig. 1 for the conditions of $K_D = 0.02\,\mu m^{-1}$ and $ut = 50\,\mu m$. The active region integrates to 0.63 and the initial generation is 0.37, adding to 1.00 in accord with a constant number of active tunnels. The dead tunnel region integrates to 1.00 in accord with Equation 6, $(0.02\,\mu m^{-1})(50\,\mu m) = 1.00$.

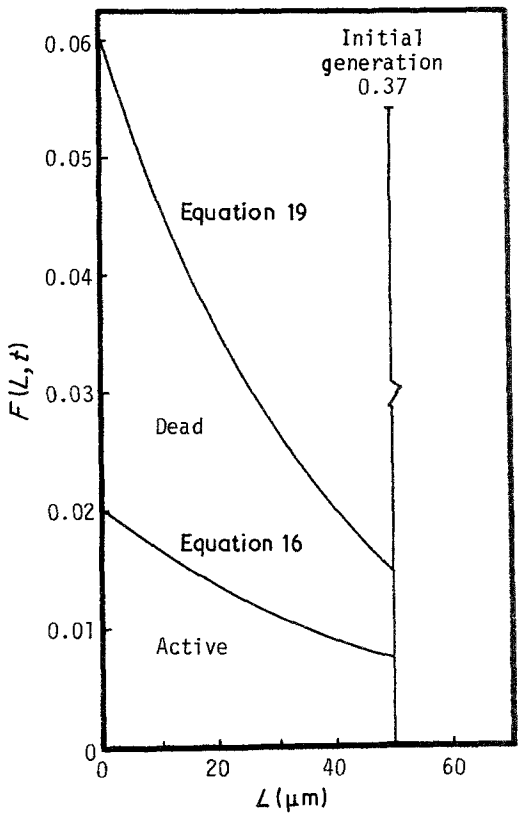

Fig. 1. Example calculated distribution of tunnel lengths for $K_D = 0.02\,\mu m^{-1}$ and $ut = 50\,\mu m$.

3. Experimental details

Tunnel length distributions were measured on SEM photographs of foil cross sections at magnifications of 600–900. A typical photograph is shown in Fig 2 for etching in 1 N HCl at 70° C at a foil current density of 200 mA cm^{-2} for a time of 50 s. Distributions were

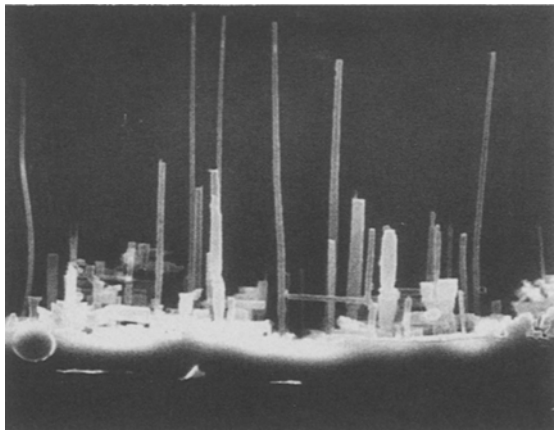

Fig. 2. Example foil cross section showing tunnel lengths: 1 N HCl, 200 mA cm^{-2}, 50 s, 720 ×.

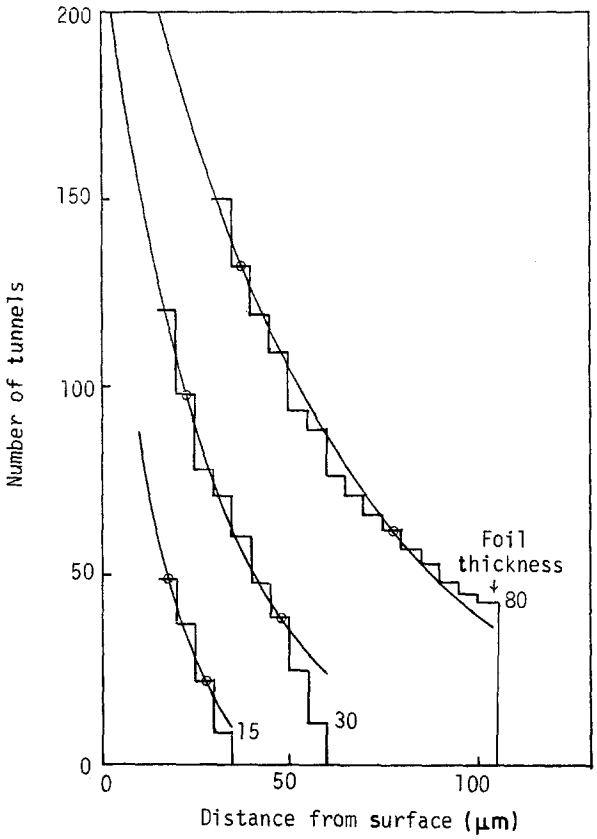

Fig. 3. Tunnel length distributions; 1 N HCl, 70° C, 200 mA cm^{-2}. Δl = 5 μm, sum of six micrographs. Numbers on curves are duration of experiments, seconds.

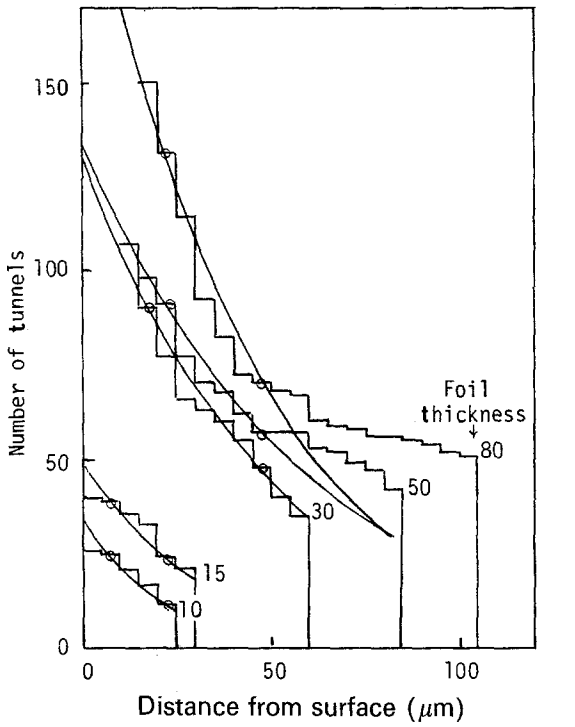

Fig. 4. Tunnel length distributions; 1 N HCl, 70° C, 200 mA cm^{-2}, Δl = 5 μm, sum of three micrographs. Numbers on curves are duration of experiments, seconds.

obtained at various times from 5 to 80 s at temperatures of 70, 80 and 90° C. Sums of tunnel lengths were taken from either three or six micrographs. Distributions are presented in Figs 3–5. The depth of the cross section in which the tunnels were counted is not known so these figures give relative distributions only.

Lengths of the longest tunnels as a function of duration of experiment from Figs 3–5 are shown in Fig. 6. The average velocities of 2.1 μm s^{-1} at 70° C and 3.5 μm s^{-1} at 80° C are in agreement with prior work [1]. No evidence is seen in Figs 3–5 of the spike of initial generation tunnels at L, which is indicated in the Fig. 3 plot. The spike, if present, should be more pronounced for the shorter duration tunnels. Lack of the spike indicates progressive nucleation early in an experiment rather than an immediate pulse of nucleation of initial generation tunnels. The remaining initial current must go to pits that do not result in tunnels. The uncounted jumble at the bottom of Fig 2 is evidence of such an occurrence. Tunnels growing parallel to the foil surface just under the surface [1] are also uncounted.

Equation 19, omitting the initial generation, is dimensionalized for correlating with the data in Figs 3–5 for which the number of tunnels for each $n\Delta l$ is known.

$$[N'_A F_T(L, t)] \simeq N'_A \{K_D \exp(-K_D l) \times [2 + K_D(ut - l)]\} \quad (20)$$

The number on the left hand side is the tunnel count

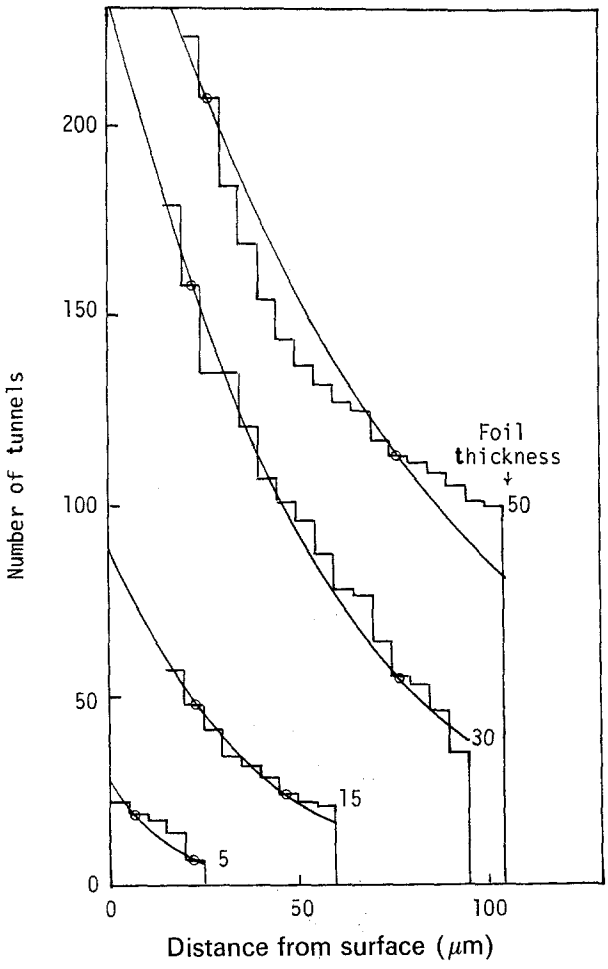

Fig. 5. Tunnel length distributions; 1 N HCl, 80° C, 200 mA cm^{-2}, Δl = 5 μm, sum of three micrographs. Numbers on curves are duration of experiments, seconds.

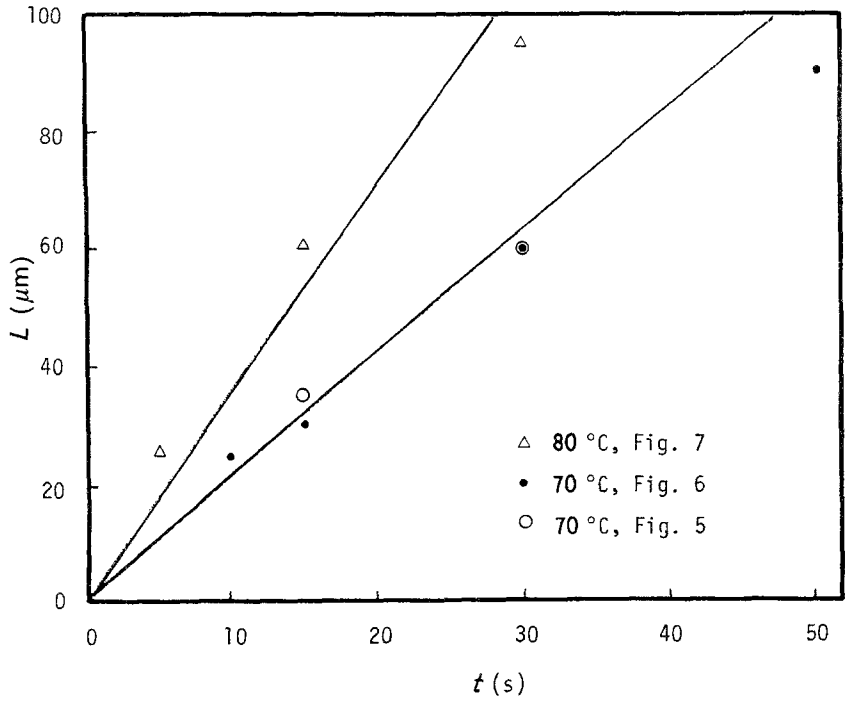

Fig. 6. Lengths of longest tunnels in Figs 3–5 as a function of duration of experiment.

at each Δl. Each distribution in Figs 3–5 was fitted at two arbitrary points, indicated by the circles on the tops of the bars, to obtain values of K_D and N'_A. Smooth curves were then plotted of Equation 20. (The numbers of tunnels in each 5-μm increment of length were divided by 5 and by either 3 or 6, the number of micrographs summed, to obtain N'_A on a consistent 1-μm unit basis per sample as for K_D and l.) Perhaps the preferential accumulation of long tunnels at long etch times, shown in Fig 3, is due to death at a critical length [2, 3].

Parameter values determined from the tunnel length distribution of Figs 3–5 and Equation 20 are given in Table 1. The total numbers of tunnels, determined by summing the number of tunnels for each 5-μm increment in Figs 3–5 and dividing by 15 or 30, are plotted in Fig. 7. The solid lines in Fig. 7 were drawn through the points at $t > 20$ s using Equation 6 dimensionalized.

$$N'_T = N'_A(1 + K_D ut) \qquad (21)$$

For 70° C, $\bar{K}_D \simeq 0.019\,\mu m^{-1}$, $u = 2.1\,\mu m\,s^{-1}$ and $K_D u \simeq 0.040\,s^{-1}$. The intercept at $t = 100$ s is therefore about five times the intercept at $t = 0$. Similarly, for 80° C, $\bar{K}_D \simeq 0.017\,\mu m$, $u = 3.5\,\mu m\,s^{-1}$ and $K_D u \simeq 0.060\,s^{-1}$. The intercept at $t = 100$ s is therefore about seven times the intercept at $t = 0$. At $t < 20$ s the numbers are considerably below the Equation 21 lines. It appears that progressive nucleation of tunnels occurs initially rather than a step increase to N'_A,

Table 1. Parameter values determined from tunnel length distributions in Figs 3–5

Fig. No.	*Temp.* (° C)	*No. of micrographs averaged*	*Duration* (s)	N'_A	K^*_D (μm^{-1})
5	70	6	15	27	(0.06)
			30	75	0.027
			80	132	0.015
6	70	3	10	25	(0.034)
			15	56	0.022
			30	199	0.015
			50	223	0.013
			80	140	(0.020)
					0.019 (average)
			5	14	(0.046)
7	80	3	15	92	0.020
			30	345	0.014
			50	589	(0.009)
					0.017 (average)
(not shown)	90	6	15	87	(0.060)
	90	3	15	155	0.021

* Values in parentheses are considered less accurate and not included in averages.

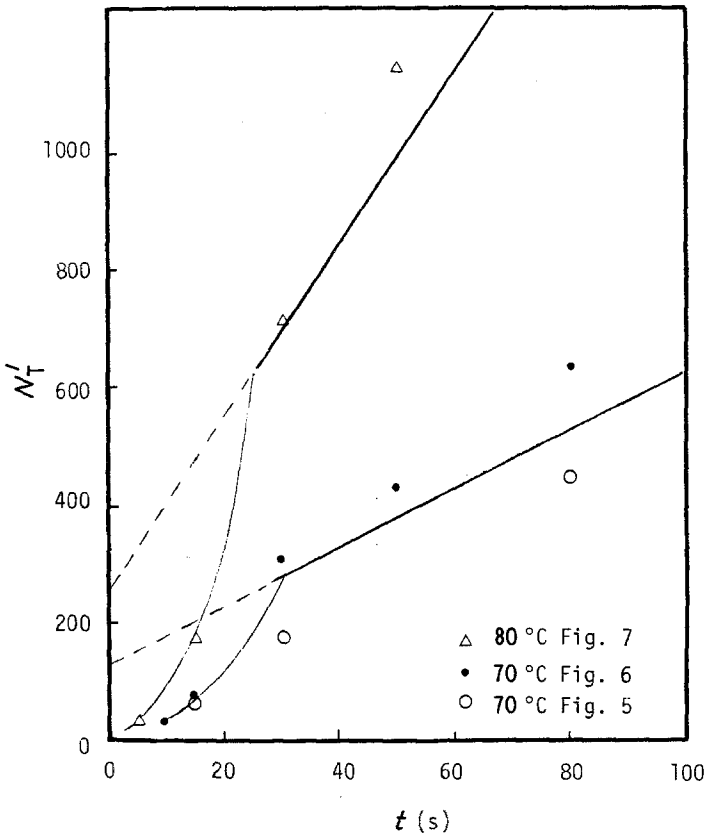

Fig. 7. Total numbers of tunnels from summation of distributions in Figs 3–5.

in agreement with lack of the initial generation spike.

Calculated values of N'_A from the fit of Equation 20 to the Figs 3–5 curves are shown in Fig. 8. Again, a progressive nucleation of active tunnels is indicated at $t < 30$ s. The plateau for the 70° C data is equal to the zero-time intercept of N'_T in Fig. 7. For 80° C, there are fewer data and the plateau N'_A in Fig. 8 and the zero-time intercept N'_T in Fig. 7 are less accurate but there is approximate agreement. The increase in number of initial active tunnels with time appears to be exponential up to about 25 s. The apparent continued increase in N'_A at $t = 50$ s may be the result of greater taper in the tunnels at 80° C.

The numbers of active tunnels on the plateau in Fig. 8 are now compared to that given by Equation 2. The foil current density was 200 mA cm^{-2} in all the experiments. At 70° C, the average current density at the ends of the tunnels is about 5.1 A cm^{-2} [1]. Average tunnel widths at 70° C measured on the micrographs from which Figs 3 and 5 were derived are about 2.1 μm. The number of active tunnels should

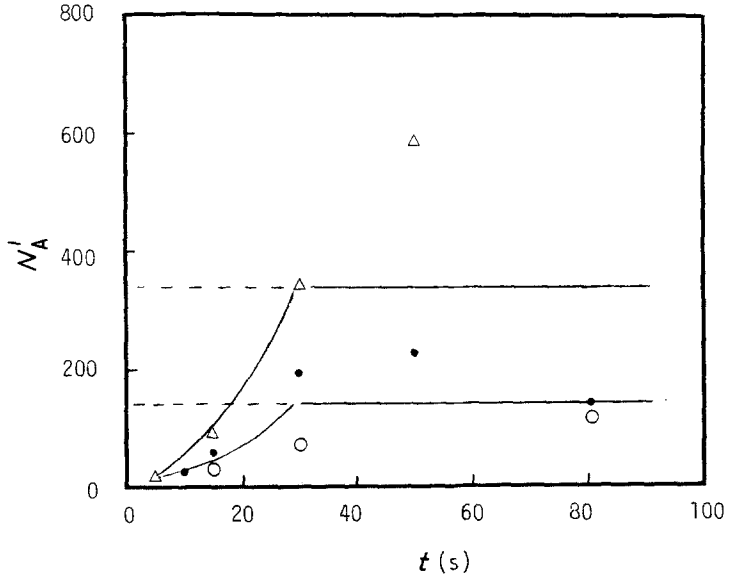

Fig. 8. Calculated values of N'_A from fit of Equation 20 to Figs 3–5 curves (same symbols as in Fig. 7).

then be

$$N_A = \frac{0.2}{(5.1)(2.1 \times 10^{-4})^2} \simeq 1 \times 10^6 \text{ cm}^{-2}$$

At 70° C the plateau number of active tunnels in Fig. 8 is $N'_A \simeq 150$. For a magnification of ~700 and a 10-cm wide micrograph the length of foil scanned is 10/700 = 0.014 cm. The depth of tunnels counted is not known but is assumed to be some fraction, ϕ, of the length scanned

$$d = \phi(0.014)$$

so that

$$N_A = \frac{150}{\phi(0.014)^2} = 7.4 \times 10^5/\phi$$

In order to agree with the estimate from Equation 2 the value of ϕ is 0.74 or the depth of tunnel population counted is about 100 μm.

No significant trend in the value of K_D in Table 1 with temperature is observed. The value of K_D appears to decrease with time or tunnel length, but it is not known whether this is a real effect.

There are several complications for actual tunnels that are not in the length distribution model as developed, and thus limit its applicability. First is the progressive tunnel initiation found in the first 25 s. Second is taper of the tunnels, particularly at 90° C. Third is penetration of the foil by long tunnels which then causes a larger number of new tunnels to initiate. Fourth is current to the walls of existing tunnels. This current density on the walls is about 10^{-3} of the average current density on the ends [4]. The total current density at the foil surface is then the sum of that to the tunnel ends and walls.

$$i_F = i_E + i_W \tag{22}$$

Equation 2 gives the value of i_E

$$i_E = N_A i_e w^2 \tag{23}$$

The value of i_W is

$$i_W = N_T i_w (4w\bar{L}) \tag{24}$$

The ratio of i_E to i_F can be obtained from Equations 22–24, Equation 5 and $i_w = 10^{-3} i_e$

$$\frac{i_E}{i_F} = \frac{1}{1 + (4 \times 10^{-3})(1 + K_D L)(\bar{L}/w)} \tag{25}$$

For an example $K_D = 0.02\,\mu\text{m}^{-1}$, $L = 100\,\mu$m, $\bar{L} = 50\,\mu$m and $w = 2\,\mu$m, the value of $i_E/i_F = 0.77$. After foil penetration this ratio can become much smaller. Because of these four complications, the short-time and the long-time values of K_D in Table 1 were not included in the averages and correlations were not attempted for longer tunnels at 90° C.

4. Conclusions

A model derived for the length distribution of corrosion etch tunnels in aluminium, tested against measured tunnel length distribution, showed the following:

(1) The model reasonably fits measured tunnel lengths with two adjustable parameters, the number of active tunnels and the death rate per unit length.

(2) At temperatures of 70–90° C tunnels die at an average rate of about 2% per μm of growth in length.

(3) At temperatures of 70 and 80° C, at which the model has validity, there is progressive nucleation of tunnels during the first 25 s.

(4) The number of active tunnels derived from the length distribution data is in approximate agreement with the value calculated from average tunnel velocities and widths.

Acknowledgements

Permission to publish the data on tunnel lengths, sponsored by KDK Corporation, is gratefully acknowledged. The interpretation of the data at Electrochemical Technology Corp. was performed under Department of Energy Contract No. DE-AC03-83ER80012. Appreciation is extended to Dr R. S. Alwitt for his interest and helpful comments.

References

[1] R. S. Alwitt, H. Uchi, T. R. Beck and R. C. Alkire, *J. Electrochem Soc.* **131** (1984) 13.

[2] K. R. Hebert, PhD Thesis, University of Illinois, February, 1985.

[3] R. S. Alwitt, T. R. Beck and K. R. Hebert, Proceedings Volume, International Conference on Localized Corrosion, June 1–5, 1987, Orlando, Florida, NACE (to be published).

[4] Fickelscher, *Dechema Mongraphien* **90** (1981) 163.